Contents lists available at http://qu.edu.iq

Al-Qadisiyah Journal for Engineering Sciences

Journal homepage: https://qjes.qu.edu.iq/

Bending, buckling, and vibration analysis of third-order shear deformation nanoplate based on modified couple stress theory

Majid Eskandari Shahraki[a]*, Mahmoud Shariati[b], Naser Asiaban[b], Mohsen Heydari Beni[c], Mohammad Reza Zamani[c], and Jafar Eskandari Jam[c]

[a] *Department of Aerospace Engineering, Faculty of Engineering, Ferdowsi University of Mashhad, Mashhad, Iran.*
[b] *Department of Mechanical Engineering, Faculty of Engineering, Ferdowsi University of Mashhad, Mashhad, Iran.*
[c] *Faculty of Materials and Manufacturing Technologies, Malek Ashtar University of Technology, Tehran, Iran*

ABSTRACT

In this paper, a third-order shear deformation rectangular nanoplate with simply supported boundary conditions is developed for bending, buckling, and vibration analysis. In order to consider the small-scale effects, the modified couple stress theory, with one length scale parameter, is used. The bending rates and dimensionless bending values under uniform surface traction and sinusoidal load, the dimensionless critical force under a uniaxial surface force in the x direction and dimensionless frequencies are all obtained for various plate's dimensional ratios and material length scale to thickness ratios. The governing equations are numerically solved. The effect of material length scale, length, width, and thickness of the nanoplate on the bending, buckling, and vibration ratios are investigated and the results are presented and discussed in detail.

1. Introduction

The atomic and molecular scale test is known as the safest method for the study of materials on small scales. In this method, the nanostructures are studied in real dimensions. Atomic force microscopy (AFM) is used to apply different mechanical loads on nanoplates and measure their responses against those loads in order to determine the mechanical properties of the nanoplate. The difficulty of controlling the test conditions at this scale, high economic costs, and time-consuming processes are some setbacks of this method. Therefore, it is used only to validate other simple and low-cost methods. Atomic simulation is another solution for studying small-scale structures. In this method, the behavior of atoms and molecules is examined by considering the intermolecular and interatomic effects on their motions, which eventually involves the total deformation of the body. In the case of large deformations and multi-atomic scale, the computational costs are too high, so this method is only used for small deformation problems.

Given the limitations of the aforementioned methods for studying nanostructures, researchers have been looking for simpler solutions for

---

* *Corresponding author.*
 E-mail address: mjdeskandari@gmail.com (Majid Eskandari Shahraki)

nanostructures. Modeling small-scale structures using continuum mechanics is another solution to this problem. There are a variety of size-dependent continuum theories that consider size effects, some of these theories are micromorphic theory, microstructural theory, micropolar theory, Kurt's theory, non-local theory, modified couple stress theory and strain gradient elasticity. All of which are the developed notion of classical field theories, which include size effects. Daghigh et al, studied the nonlocal bending and buckling of agglomerated CNT-Reinforced composite nanoplates. They investigated the effect of the parameters, such are degree of agglomeration, nonlocal material scale parameter, temperature, foundation properties, volume fraction of CNTs, and length-to-thickness aspect ratio for the plate [19].

Daikh et al, studied A novel nonlocal strain gradient Quasi-3D bending analysis of sigmoid functionally graded sandwich nanoplates. They investigated the effect of the elastic foundation models, sigmoidal distribution index constant, configuration of sandwich plate, material and length nanoscales, boundary conditions on the static deflection [20]. Ruocco et al, studied the buckling analysis of elastic–plastic nanoplates resting on a Winkler–Pasternak foundation based on nonlocal third-order plate theory. They investigated the effect of geometrical, constitutive, and nonlocal parameters on the critical behavior of plates with different boundary conditions [21]. Banh-Thien et al, studied the buckling analysis of non-uniform thickness nanoplates in an elastic medium using the isogeometric analysis. They discretized the governing equation into algebraic equations and solved by using IGA procedure to determine the critical buckling load. By using the non-uniform rational B-splines, IGA easily satisfies the required continuity of the partial differential equations in buckling analysis [22].

In this paper, size-dependent nanoplate model is developed to account for the size effect. Hamilton principle is used to derive the equations of motion based on the mentioned theories (i.e., modified couple stress and third order shear deformation theories). In order to investigate the effects of material length scale parameter on deflection, buckling and frequency, analytical solution for a static problem is obtained for a simply supported plate and results are discussed.

2. Modified coupled stress theory

In 2002 Yang et al. [1] proposed a modified couple stress model by modifying the theory proposed by Toppin [2], Mindlin and Thursten [3], Quitter [4] and Mindlin [5] in 1964. The modified couple stress theory consists of one material length scale parameter for projection of the size effect, whereas the classical couple stress theory has two material length scale parameters. In the modified couple stress theory the strain energy density in the three-dimensional vertical coordinates for a body bounded by the volume V and the area Ω [6], is expressed as the follows:

$$U = \frac{1}{2}\int_v (\sigma_{ij}\varepsilon_{ij} + m_{ij}\chi_{ij})dV \quad i,j = 1,2,3 \tag{1}$$

Were,

$$\varepsilon_{ij} = \frac{1}{2}(u_{i,j} + u_{j,i}) , \chi_{ij} = \frac{1}{2}(\theta_{i,j} + \theta_{j,i}) \tag{2}$$

χ_{ij} and ε_{ij} are the symmetric parts of the curvature and strain tensors and θ_i and u_i are the displacement and the rotational vectors, respectively.

$$\theta = \frac{1}{2} Curl\, u \tag{3}$$

σ_{ij}, the stress tensor, and m_{ij} the deviatory part of the couple stress tensor, are defined as:

$$\sigma_{ij} = \lambda\varepsilon_{kk}\delta_{ij} + 2\mu\varepsilon_{ij} \quad , \quad m_{ij} = 2\mu\, l^2\chi_{ij} \tag{4}$$

Where λ and μ are the lame constants, δ_{ij} is the Kronecker delta and l is the material length scale parameter. From Equations (2) and (4) it can be seen that χ_{ij} and m_{ij} are symmetric.

3. Third order shear deformation nanoplate model

In **Fig.1** an isotropic rectangular nanoplate with length a, width b and thickness h are shown.
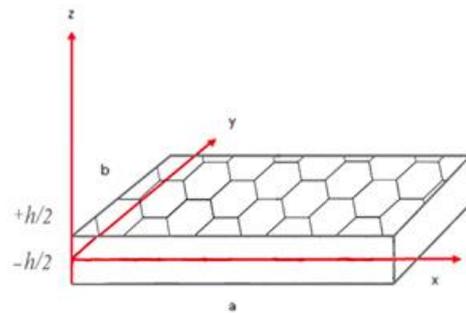
Figure 1. A schematic of the nanoplate and axes

The displacement equations for the third order shear deformation nanoplate are defined as (According to the Reddy shear theory):

$$u_1(x,y,z,t) = z\,\varphi_x(x,y,t) - \frac{4}{3}\left(\frac{1}{h}\right)^2 z^3\left(\frac{\partial w(x,y,t)}{\partial x} + \varphi_x(x,y,t)\right)$$

$$u_2(x,y,z,t) = z\varphi_y(x,y,t) - \frac{4}{3}\left(\frac{1}{h}\right)^2 z^3\left(\frac{\partial w(x,y,t)}{\partial y} + \varphi_y(x,y,t)\right) \tag{5}$$

$$u_3(x,y,z,t) = w(x,y,t)$$

Where φ_x and φ_y are rotation of the normal vector around the x, y and w are the displacement of the middle surface at the z axes. The symmetric part of curvature tensor, strain and stress tensor and rotation vector for third order shear deformation nanoplate model are as follows:

$$
\begin{aligned}
\varepsilon_{xx} &= z\frac{\partial\varphi_x}{\partial x} - \frac{4}{3}\left(\frac{1}{h}\right)^2 z^3\left(\frac{\partial^2 w}{\partial x^2} + \frac{\partial\varphi_x}{\partial x}\right)\\
\varepsilon_{yy} &= z\frac{\partial\varphi_y}{\partial y} - \frac{4}{3}\left(\frac{1}{h}\right)^2 z^3\left(\frac{\partial^2 w}{\partial y^2} + \frac{\partial\varphi_y}{\partial y}\right)\\
\varepsilon_{zz} &= 0\\
\varepsilon_{xy} &= \varepsilon_{yx} = \frac{1}{2}z\left(\frac{\partial\varphi_x}{\partial y} + \frac{\partial\varphi_y}{\partial x}\right)\\
&\quad - \frac{2}{3}\left(\frac{1}{h}\right)^2 z^3\left(\frac{\partial\varphi_x}{\partial y} + \frac{\partial\varphi_y}{\partial x} + 2\frac{\partial^2 w}{\partial x\partial y}\right)\\
\varepsilon_{xz} &= \varepsilon_{zx} = \left(\frac{1}{2} - 2\left(\frac{z}{h}\right)^2\right)\left(\frac{\partial w}{\partial x} + \varphi_x\right)\\
\varepsilon_{yz} &= \varepsilon_{zy} = \left(\frac{1}{2} - 2\left(\frac{z}{h}\right)^2\right)\left(\frac{\partial w}{\partial y} + \varphi_y\right)
\end{aligned}
\tag{6}
$$

$$\theta_x = \frac{\partial w}{\partial y} - \left(\frac{1}{2} - 2\left(\frac{z}{h}\right)^2\right)\left(\frac{\partial w}{\partial y} + \varphi_y\right)$$

$$\theta_y = -\frac{\partial w}{\partial x} + \left(\frac{1}{2} - 2\left(\frac{z}{h}\right)^2\right)\left(\frac{\partial w}{\partial x} + \varphi_x\right)$$

$$\theta_z = \frac{1}{2}\left(z - \frac{4}{3}\left(\frac{1}{h}\right)^2 z^3\right)\left(\frac{\partial \varphi_y}{\partial x} - \frac{\partial \varphi_x}{\partial y}\right)$$

(7)

$$x_{xx} = \frac{\partial^2 w}{\partial x\,\partial y} - \left(\frac{1}{2} - 2\left(\frac{z}{h}\right)^2\right)\left(\frac{\partial^2 w}{\partial x\,\partial y} + \frac{\partial \varphi_y}{\partial x}\right)$$

$$x_{yy} = -\frac{\partial^2 w}{\partial x\partial y} + \left(\frac{1}{2} - 2\left(\frac{z}{h}\right)^2\right)\left(\frac{\partial \varphi_x}{\partial y} + \frac{\partial^2 w}{\partial x\partial y}\right)$$

$$x_{zz} = \left(\frac{1}{2} - 2\left(\frac{z}{h}\right)^2\right)\left(\frac{\partial \varphi_y}{\partial x} - \frac{\partial \varphi_x}{\partial y}\right)$$

$$x_{xy} = \frac{1}{2}\left(\frac{\partial^2 w}{\partial y^2} - \frac{\partial^2 w}{\partial x^2}\right)$$
$$+ \left(\frac{1}{4} - \left(\frac{z}{h}\right)^2\right)\left(\frac{\partial^2 w}{\partial x^2} + \frac{\partial \varphi_x}{\partial x}\right.$$
$$\left. - \frac{\partial^2 w}{\partial y^2} - \frac{\partial \varphi_y}{\partial y}\right)$$

$$x_{xz} = \frac{1}{4}\left(z - \frac{4}{3}\left(\frac{1}{h}\right)^2 z^3\right)\left(\frac{\partial^2 \varphi_y}{\partial x^2} - \frac{\partial^2 \varphi_x}{\partial y\,\partial x}\right)$$
$$+ 2z\left(\frac{1}{h}\right)^2\left(\frac{\partial w}{\partial y} + \varphi_y\right)$$

$$x_{yz} = -2z\left(\frac{1}{h}\right)^2\left(\frac{\partial w}{\partial x} + \varphi_x\right)$$
$$+ \frac{1}{4}\left(z - \frac{4}{3}\left(\frac{1}{h}\right)^2 z^3\right)\left(\frac{\partial^2 \varphi_y}{\partial x\partial y}\right.$$
$$\left. - \frac{\partial^2 \varphi_x}{\partial y^2}\right)$$

(8)

$$\sigma_{xx} = (\lambda + 2\mu)\varepsilon_{xx} + \lambda\varepsilon_{yy}$$

$$\sigma_{yy} = \lambda\varepsilon_{xx} + (\lambda + 2\mu)\varepsilon_{yy}$$

$$\sigma_{zz} = \lambda(\varepsilon_{xx} + \varepsilon_{yy})$$

$$\sigma_{yx} = \sigma_{xy} = 2\mu\,\varepsilon_{xy}$$

$$\sigma_{xz} = \sigma_{zx} = 2\mu\,\varepsilon_{xz}$$

$$\sigma_{yz} = \sigma_{zy} = 2\mu\,\varepsilon_{yz}$$

(9)

The variation of strain energy is expressed as:

$$\delta U = \int_v (\sigma_{xx}\,\delta\,\varepsilon_{xx} + \sigma_{yy}\,\delta\varepsilon_{yy} + 2\sigma_{xy}\,\delta\,\varepsilon_{xy} +$$
$$2\sigma_{xz}\,\delta\,\varepsilon_{xz} + 2\sigma_{yz}\,\delta\,\varepsilon_{yz} + m_{xx}\,\delta\,x_{xx} + m_{yy}\,\delta x_{yy}$$
$$+ m_{zz}\,\delta x_{zz}$$

(10)

$$+2m_{xy}\,\delta x_{xy} + 2m_{xz}\,\delta x_{xz} + 2m_{yz}\,\delta\,x_{yz})dV$$

After substituting and simplify result in Eq. (11):

$$\delta U = \int_V \ (E_1\delta w_{,xx} + E_2\,\delta w_{,yy} + E_3\,\delta w_{,xy} + E_4\delta\,w_{,x}$$

$$+ E_5\,\delta\,w_{,y} + E_6\,\delta\,\varphi_{x,yy} + E_7\delta\,\varphi_{y,xx} + E_8\,\delta\,\varphi_{y,xy}$$
$$+ E_9\,\delta\varphi_{x,yx}$$

$$+ E_{10}\,\delta\,\varphi_{x,x} + E_{11}\,\delta\varphi_{y,y} + E_{12}\delta\varphi_{x,y} + E_{13}\,\delta\,\varphi_{y,x}$$
$$+ E_{14}\,\delta\varphi_x$$

$$+ E_{15}\,\delta\varphi_y)dV$$

(11)

The coefficients of variables E_i are obtain In the appendix A.

$$I_i = \int_{-\frac{h}{2}}^{\frac{h}{2}} Z^i\ dz\ (i = 0,1,2,n-1,n,n+1,2n-4,2n$$
$$-2,2n)$$

(12)

4. Buckling load

For a rectangular plate with length a, width b and thickness h with the forces P_x, P_y, P_{xy} and external force $q(x,y)$ the buckling force equation can be written as [7, 8]:

$$P_x \frac{\partial^2 w}{\partial x^2} + 2P_{xy}\,\frac{\partial^2 w}{\partial x\partial y} + P_y \frac{\partial^2 w}{\partial y^2} = q(x,y)$$

(13)

5. Virtual work of the external forces

In this kind of problems, the virtual work of three kinds of external forces are included in the solutions, if the middle-plane and the middle-perimeter of the plate are shown as Ω and Γ respectively, these virtual works are [9]:

1. The virtual work done by the body forces, which is applied on the volume V= $\Omega \times$ (- h/2, h/2).

2. The virtual work done by the surface tractions at the upper and lower surfaces (Ω).

3. The virtual work done by the shear tractions on the lateral surfaces, S= $\Gamma \times$ (- h/2, h/2).

If (f_x, f_y, f_z) are the body forces, (c_x, c_y, c_z) are the body couples, (q_x, q_y, q_z) are the forces acting on the Ω plane, (t_x, t_y, t_z) are the Cauchy's tractions and (S_x, S_y, S_z) are surface couples the Variation of the virtual work is expressed as:

$$\delta w = -\left[\iint_\Omega (f_x\delta u + f_y\delta V + f_z\delta w + q_x\delta u + q_y\delta V + q_z\delta w\right.$$
$$+ c_x\delta\theta_x + c_y\,\delta\theta_y + c_z\delta\theta_z)\,dx\,dy$$
$$+ \int_\Gamma (t_x\delta u + t_y\delta V + t_z\delta w + s_x\theta_x$$
$$\left. + s_y\delta\theta_y + s_z\delta\theta_z)d\Gamma\right]$$

(14)

Given that only external force q_z is applied in this research, virtual work is as follows:

$$\delta w = \int_0^a \int_0^b q(x,y)\delta w(x,y)dx\,dy \tag{15}$$

The kinetic energy variation is expressed as follows:

$$\delta T = \int_A \int_{-\frac{h}{2}}^{\frac{h}{2}} \rho(\dot{u}_1\delta\dot{u}_1 + \dot{u}_2\delta\dot{u}_2 + \dot{u}_3\delta\dot{u}_3)dA\,dz \tag{16}$$

Where ρ is density. In this study, the equation of motion is derived by Hamilton's principle. This principle can be expressed as [10]:

$$\int_0^T \big(\delta T - (\delta U - \delta w)\big)dt = 0 \tag{17}$$

In which T is the kinetic energy, U is the strain energy and W is the work of external forces.

6. The final equation of the nanoplate by applying buckling and external force

By applying the Hamilton's principle, the main equations are obtained as follows:

$$\left[\int_{-h/2}^{h/2}\left(\frac{\partial^2 E_1}{\partial x^2} - \frac{\partial E_4}{\partial x} + \frac{\partial^2 E_2}{\partial y^2} + \frac{\partial^2 E_3}{\partial x\partial y} - \frac{\partial E_5}{\partial y}\right)dz\right] + P_x\frac{\partial^2 w}{\partial x^2}$$

$$+ 2P_{xy}\frac{\partial^2 w}{\partial x\partial y}$$

$$+P_y\frac{\partial^2 w}{\partial y^2} = q(x,y) + \rho I_0 w_{,tt} - C_6{}^2\rho I_6\left(\frac{\partial^2 w}{\partial x^2} + \frac{\partial^2 w}{\partial y^2}\right)_{,tt}$$

$$+ C_6\,\rho J_4\left(\frac{\partial\varphi_x}{\partial x} + \frac{\partial\varphi_y}{\partial y}\right)_{,tt}$$

$$\int_{-h/2}^{h/2}\left(\frac{\partial^2 E_6}{\partial y^2} + \frac{\partial^2 E_9}{\partial x\partial y} - \frac{\partial E_{12}}{\partial y} - \frac{\partial E_{10}}{\partial x} + F_{14}\right)dz = \rho K_2\varphi_{x,tt}$$

$$- C_6\,\rho J_4\left(\frac{\partial w}{\partial x}\right)_{,tt}$$

$$\int_{-h/2}^{h/2}\left(\frac{\partial^2 E_7}{\partial x^2} - \frac{\partial E_{13}}{\partial x} + \frac{\partial^2 E_8}{\partial x\partial y} - \frac{\partial E_{11}}{\partial y} + E_{15}\right)dz$$

$$= \rho K_2\varphi_{y,tt} - C_6\,\rho J_4\left(\frac{\partial w}{\partial y}\right)_{,tt} \tag{18}$$

$$J_4 = I_4 - C_6\,I_6$$
$$K_2 = I_2 - 2C_6\,I_4 - C_6{}^2 I_6 \tag{19}$$

7. Obtaining third order shear deformation nanoplate equations in the general state (including bending, buckling and vibrations)

The general equations of the third order shear deformation nanoplate will be obtained as follows:

The coefficients of variables from D_i are obtained in the appendix B.

$$D_1\frac{\partial^4 w}{\partial x^2\,\partial y^2} + D_2\frac{\partial^4 w}{\partial x^4} + D_2\frac{\partial^4 w}{\partial y^4} + D_3\frac{\partial^2 w}{\partial x^2} + D_3\frac{\partial^2 w}{\partial y^2}$$

$$+ D_4\frac{\partial^3 \varphi_x}{\partial x^3} + D_4\frac{\partial^3 \varphi_x}{\partial x\,\partial y^2} + D_4\frac{\partial^3 \varphi_y}{\partial y\,\partial x^2}$$

$$+ D_3\frac{\partial\varphi_x}{\partial x} + D_3\frac{\partial\varphi_y}{\partial y} + D_4\frac{\partial^3 \varphi_y}{\partial y^3}$$

$$+ P_x\frac{\partial^2 w}{\partial x^2} + 2P_{xy}\frac{\partial^2 w}{\partial x\partial y}$$

$$+P_y\frac{\partial^2 w}{\partial y^2} = q(x,y) + \rho h\frac{\partial^2 w}{\partial t^2} - D_{11}\left(\frac{\partial^4 w}{\partial x^2\,\partial t^2} + \frac{\partial^4 w}{\partial y^2\,\partial t^2}\right)$$

$$+ D_{12}\left(\frac{\partial^3 \varphi_x}{\partial x\,\partial t^2} + \frac{\partial^3 \varphi_y}{\partial y\,\partial t^2}\right) \tag{20}$$

$$-D_4\frac{\partial^3 w}{\partial x\,\partial y^2} + D_5\frac{\partial^2 \varphi_y}{\partial y\,\partial x} + D_6\frac{\partial^2 \varphi_x}{\partial y^2} + D_7\frac{\partial^4 \varphi_y}{\partial x\,\partial y^3} - D_7\frac{\partial^4 \varphi_x}{\partial y^4}$$

$$+ D_7\frac{\partial^4 \varphi_y}{\partial y\,\partial x^3} - D_7\frac{\partial^4 \varphi_x}{\partial y^2\,\partial x^2} - D_3\frac{\partial w}{\partial x}$$

$$- D_3\varphi_x - D_4\frac{\partial^3 w}{\partial x^3} + D_8\frac{\partial^2 \varphi_x}{\partial x^2}$$

$$= -D_{12}\frac{\partial^3 w}{\partial x\,\partial t^2} + D_{13}\frac{\partial^2 \varphi_x}{\partial t^2} \tag{21}$$

$$-D_4\frac{\partial^3 w}{\partial y\,\partial x^2} + D_9\frac{\partial^2 \varphi_x}{\partial y\,\partial x} + D_{10}\frac{\partial^2 \varphi_y}{\partial x^2} + D_7\frac{\partial^4 \varphi_y}{\partial x^4} + D_7\frac{\partial^4 \varphi_y}{\partial x^2\,\partial y^2}$$

$$- D_7\frac{\partial^4 \varphi_x}{\partial y\,\partial x^3} - D_7\frac{\partial^4 \varphi_x}{\partial x\,\partial y^3} - D_4\frac{\partial^3 w}{\partial y^3}$$

$$- D_3\frac{\partial w}{\partial y} - D_3\varphi_y + D_8\frac{\partial^2 \varphi_y}{\partial y^2}$$

$$= -D_{12}\frac{\partial^3 w}{\partial y\,\partial t^2} + D_{13}\frac{\partial^2 \varphi_y}{\partial t^2} \tag{22}$$

8. Navier Solution Method

The Navier solution method is applicable to rectangular plates with simply supported boundary conditions on all edges. The displacement functions of the middle surface can be expanded in the forms of double trigonometric series as follows [9, 11]:

$$W(x,y,t) = \sum_{m=1}^{\infty}\sum_{n=1}^{\infty} W_{mn}\sin\alpha x\,\sin\beta y\,e^{i\omega t}$$

$$\varphi_x(x,y,t) = \sum_{m=1}^{\infty}\sum_{n=1}^{\infty} X_{mn}\cos\alpha x\,\sin\beta y\,e^{i\omega t}$$

$$\varphi_y(x,y,t) = \sum_{m=1}^{\infty}\sum_{n=1}^{\infty} y_{mn}\sin\alpha x\,\cos\beta y\,e^{i\omega t} \tag{23}$$

load can also be calculated from the following equation:

$$q = \sum_{m=1}^{\infty}\sum_{n=1}^{\infty} Q_{mn}\sin\alpha x\,\sin\beta y\,e^{i\omega t} \tag{24}$$

$$Q_{mn} = \frac{4}{ab}\int_0^a\int_0^b q(x,y)\sin\alpha x\,\sin\beta y\,dx\,dy$$

Where $\alpha = \frac{\pi m}{a}$, $\beta = \frac{\pi n}{b}$, $i = \sqrt{-1}$

9. Obtaining the matrix of third order shear deformation nanoplate equations

After solving the equation using the Navier method the general matrix of third order shear deformation nanoplate equations will be obtained as follows:

$$\left(\begin{bmatrix} R_1 & R_2 & R_3 \\ R_4 & R_5 & R_6 \\ R_7 & R_8 & R_9 \end{bmatrix} - \omega^2 \begin{bmatrix} G_1 & G_2 & G_3 \\ G_4 & G_5 & G_6 \\ G_7 & G_8 & G_9 \end{bmatrix} \right) \begin{bmatrix} w_{mn} \\ X_{mn} \\ y_{mn} \end{bmatrix} = \begin{bmatrix} Q_{mn} \\ 0 \\ 0 \end{bmatrix} \qquad (25)$$

The coefficients of variables R_i and G_i are obtained In the appendix C.

In this paper, graphene is considered for the material of the nanoplate. A single layer graphene sheet has the following properties [10]:

$E = 1.06 TPa, v = 0.25, h = 0.34nm, \rho = 2250 \, kg/_{m^3}$

Also, the relationship between E, μ and ν can be written as:

$$\lambda = \frac{vE}{(1+v)(1-2v)} \quad , \mu = \frac{E}{2(1+v)}$$

Where E is the Young modulus and μ and λ are Lame coefficients [12]. Also, q = 1N / m^2.

10. Results and discussion

The results are obtained using MATLAB software. All boundary conditions are also considered as simply supported. Table 1 compares the dimensionless static deflections of nanoplates subjected to a sinusoidal load. According to the table 1, the dimensionless static deflections of Kirchhoff nanoplate has the highest value and the Mindlin nanoplate has the lowest. Table 2 compares the dimensionless static deflections of the third order shear deformation nanoplate subjected to the uniform load for different value of length/width ratio. It is observed that except classical mode (l =0), by increasing the length scales parameter/thickness ratio, the dimensionless static deflections is decreased. Also by increasing the length/width ratio, it is increased.

Table 1. Comparison of dimensionless static deflections of nanoplates subjected to a sinusoidal load for different values of a/b (a / h = 30, q = 1e-18N / nm^2, l / h = 1).

a/b	Kirchhoff plate	Mindlin plate	Third order Shear deformation plate	N order shear deformation plate (n=5)
1.0	0.2	0.07226	0.19912	0.19907
1.5	0.2	0.07212	0.19927	0.19923
2.0	0.2	0.07204	0.19935	0.19931

Table 2. Dimensionless static deflections of the third order shear deformation nanoplate subjected to the uniform load for different value of length/width ratio (q = 1e-18 N / nm^2 a / h = 30)

a/b	l/h			
	0.0	0.5	1.0	2.0
1.0	1.00000	0.49874	0.19922	0.05856
1.5	1.00000	0.49911	0.19945	0.05864
2.0	1.00000	0.49923	0.19952	0.05866

Table 3 compares the static deflections of the third order shear deformation nanoplate subjected to the sinusoidal load for different values of length/width ratio. It is observed that by increasing the length scales parameter/thickness ratio, the static deflections is decreased. Also by increasing the length/width ratio, it is increased.

Table 3. Static deflections of the third order shear deformation nanoplate subjected to the sinusoidal load for different values of length/width ratio (q = 1e-18 N / nm ^ 2 a / h = 30)

a/b	l/h			
	0.0	0.5	1.0	2.0
1.0	07.0630	03.5215	1.4064	0.4134
1.5	14.2905	07.1284	2.8477	0.8371
2.0	21.1039	10.5297	4.2070	1.2367

Figure 2 shows the dimensionless critical buckling load of the third order shear deformation nanoplate for biaxial buckling and different value of length/thickness ratio. It is observed that by increasing the length scales parameter/thickness ratio the dimensionless critical buckling load is increased. Also except for the classical mode (l = 0) by increasing the length/ thickness ratio, it is decreased. Dimensionless critical buckling load for uniaxial buckling and different nanoplate dimensionless critical buckling load for uniaxial buckling and different nanoplate.
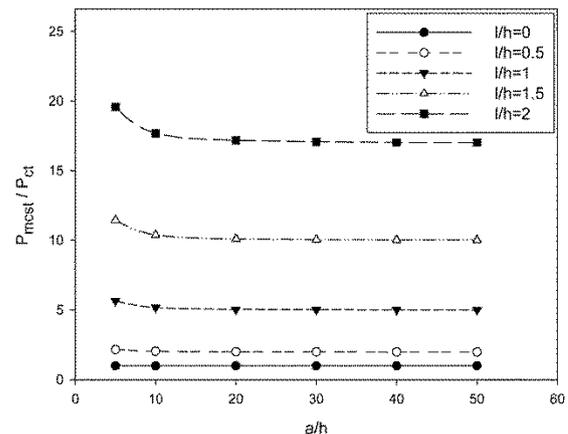
Figure 2. Comparison of the dimensionless critical buckling load of the third order shear deformation nanoplate for biaxial buckling and different values of length/thickness ratio (a / b = 1)

Table 4 compares the dimensionless critical buckling load for uniaxial buckling and different nanoplate. According to Table 4:

- By increasing the length/thickness ratio of the Mindlin nanoplate, the dimensionless critical buckling load for uniaxial buckling is increased.
- By increasing the length/thickness ratio of the third and fifth order shear deformation nanoplates, the dimensionless critical buckling load for uniaxial buckling is slightly decreased.
- By increasing the length/thickness ratio of the Kirchhoff nanoplate, the dimensionless critical buckling load for uniaxial buckling is fixed.

Table 4. Dimensionless critical buckling load for uniaxial buckling and different nanoplates (a / b = 1, l / h = 1)

a/h	Kirchhoff nanoplate	Mindlin nanoplate	Third order shear deformation nanoplate	N order shear deformation nanoplate (n=5)
05	5.0000	10.1594	5.6521	5.6937
10	5.0000	12.8100	5.1723	5.1826
20	5.0000	13.6820	5.0437	5.0463
30	5.0000	13.8568	5.0195	5.0206
40	5.0000	13.9191	5.0110	5.0116
50	5.0000	13.9481	5.0070	5.0074

Figure 3 shows the critical buckling load of the third order shear deformation nanoplate for uniaxial buckling and different value of length/thickness ratio. It is observed that by increasing the length scales parameter/thickness ratio the critical buckling load is increased. Also, by increasing the length/ thickness ratio, it is decreased.
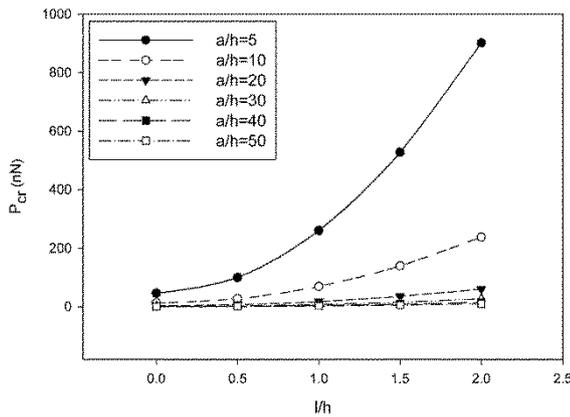
Figure 3. Comparison of the critical buckling load of the third order shear deformation nanoplate for uniaxial buckling and different values of length/thickness ratio (a / b = 1)

Table 5. shows the dimensionless critical buckling load of the third order shear deformation nanoplate for biaxial buckling and different buckling modes. It is observed that by increasing the length scales parameter/thickness ratio the dimensionless critical buckling load is increased. Also, for first mode, it is minimum.

Table 5. Comparison of the dimensionless critical buckling load of the third order shear deformation nanoplate for biaxial buckling and different buckling modes (a/h = 30 and a/b = 1)

Mode	l/h			
	0.0	0.5	1.0	2.0
p_{11}	1.0000	2.0050	5.0195	17.0765
p_{12}	1.0000	2.0125	5.0486	17.1908
p_{21}	1.0000	2.0125	5.0486	17.1908
p_{22}	1.0000	2.0199	5.0774	17.3044

Figures 4 to 7 show the dimensionless frequencies (ω_{11} / ω_{ct}- ω_{12} / ω_{ct}- ω_{21} / ω_{ct}- ω_{22} / ω_{ct}) of the third order shear deformation nanoplate for different values of length/thickness ratio. It is observed that by increasing the length scales parameter/thickness ratio, the dimensionless frequencies are increased. Also except for classical mode (l = 0) by increasing the length/ thickness ratio, it is decreased. As well as for first mode, it is minimum.
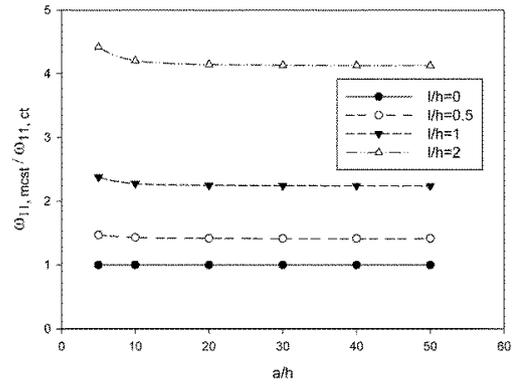
Figure. 4. Comparison of the dimensionless frequencies (ω_{11}) of the third order shear deformation nanoplate for different values of length/thickness ratio (a / b = 1, h = 0.34)
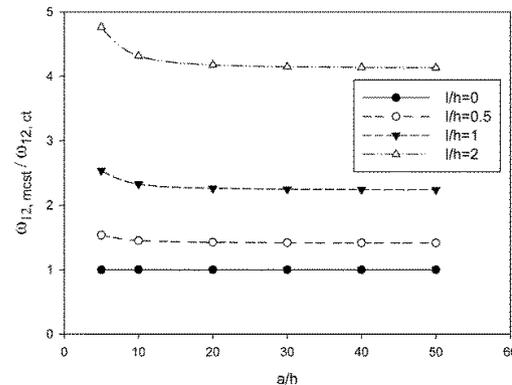
Figure 5. Comparison of the dimensionless frequencies (ω_{12}) of the third order shear deformation nanoplate for different values of length/thickness ratio (a / b = 1, h = 0.34)
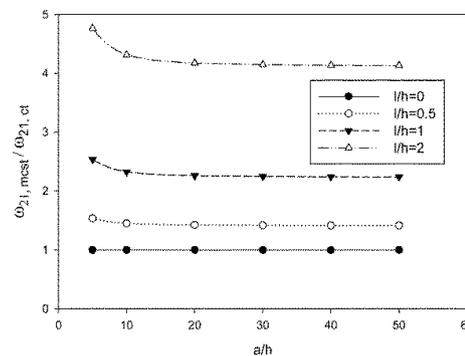
Figure 6. Comparison of the dimensionless frequencies (ω_{21}) of the third order shear deformation nanoplate for different values of length/thickness ratio (a / b = 1, h = 0.34)
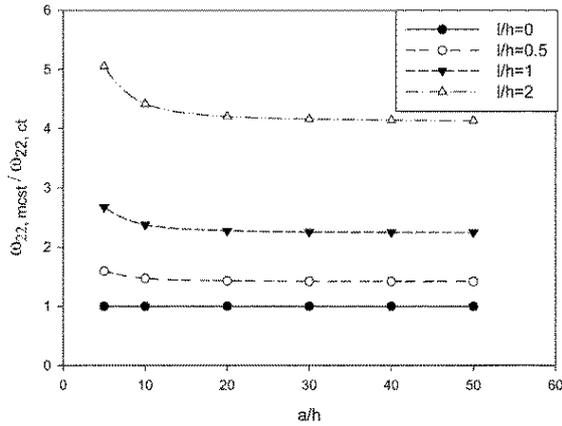
Figure 7. Comparison of the dimensionless frequencies (ω_{22}) of the third order shear deformation nanoplate for different values of length/thickness ratio (a / b = 1, h = 0.34)

Table 6. Comparison of the frequencies of the third order shear deformation nanoplate for different value of length scales parameter /thickness ratio (MHz) (a / b = 1, a / h = 30)

Mode	l/h			
	0	0.5	1	2
ω_{11}	13.9441	19.7447	31.2407	57.6223
ω_{12}	34.6497	49.1546	77.8533	143.6613
ω_{21}	34.6497	49.1546	77.8533	143.6613
ω_{22}	55.1098	78.3225	124.1752	229.2384
ω_{33}	121.6342	173.8911	276.5826	511.3107

Table 7. Comparison of frequencies for the different nanoplates (a / b = 0.5, l / h = 1)

Mode	a/h		
	20	30	40
Mindlin plate			
ω_{11}	280.4153	128.0217	72.7219
ω_{21}	436.5378	202.1703	115.4757
ω_{12}	860.2980	413.9252	240.0504
ω_{22}	988.5087	481.2484	280.4153
Kirchhoff plate			
ω_{11}	175.2090	78.0917	43.9704
ω_{21}	279.4825	124.7767	70.2985
ω_{12}	588.5668	264.0744	149.0415
ω_{22}	690.3772	310.2573	175.2090
Third order shear deformation plate			
ω_{11}	174.0385	77.8533	43.8941
ω_{12}	276.5826	124.1752	70.1049
ω_{21}	576.6542	261.4753	148.1887
ω_{22}	674.3836	306.7113	174.0385

Table 6 shows that by increasing the length scales parameter/thickness ratio, the frequencies of different modes (ω_{11}-ω_{12}-ω_{21}-ω_{22}) are increased. Table 7. Shows the frequency of different modes (ω_{11}-ω_{12}-ω_{21}-ω_{22}) for different nanoplates. According to the table, the frequency of Mindlin nanoplate is maximum and for third order shear deformation nanoplate is minimum.

The results of this paper have been verified by being compared to references [13-18] and good agreement is attained between the results.

11. Conclusion

In this paper bending, buckling and vibrations of the third order shear deformation nanoplate was studied. As shown in tables and figures, by increasing the length scales parameter/thickness ratio, the dimensionless static deflection of nanoplate subjected to a sinusoidal load is decreased. It is also increased by increasing the length/width ratio.

By increasing the length scales parameter/thickness ratio the dimensionless critical buckling load for biaxial buckling is increased. It's also observed that this value decreases by increasing the length/ thickness ratio, except for the classical mode. As discussed before, by increasing the length scales parameter/thickness ratio, the dimensionless frequencies are increased, except for the classical mode (l = 0), which is decreased by increasing the length/ thickness ratio. And the minimum value of this parameter is obtained for the first mode.

Authors' contribution
All authors contributed equally to the preparation of this article.

Declaration of competing interest
The authors declare no conflicts of interest.

REFERENCES

[1] F. Yang, A. C. M. Chong, D. C. C. Lam and P. Tong, "Couple stress Based Strain gradient theory for elasticity," Int.J.Solids Struct.39, 2731–2743(2012).
[2] R. A. Toupin, "Elastic materials with couple stresses," Archive for Rational Mechanics and Analysis, 11(1), 385–414(1962).
[3] R. D. Mindlin and H. F. Tiersten, "Effects of couple-stresses in linear elasticity," Archive for Rational Mechanics and Analys, 11(1), 415–448(1962).
[4] W. T. Koiter, "Couple stresses in the theory of elasticity," I & II. Philosophical Transactions of the Royal Society of London B, 67, 17–44(1964).
[5] R. D. Mindlin, "Micro-structure in linear elasticity, " Archive for Rational Mechanics and Analys, 16(1), 51–78(1964).
[6] G. C. Tsiatas, "A new kirchhoff model based on a modified couple stress theory," International Journal of solids and structures, 46(13), 2757-2764(2009).
[7] B. Wang, S. Zhou, J. Zhao, and X. Chen, "A size-dependent kirchhoff micro-plate model based on strain gradient elasticity theory," European Journal of mechanics A/Solids, 30(4), 517-524(2011).
[8] A. Farajpour, A. R. Shahidi, M. Mohammadi and M. Mahzoon, "Buckling of orthotropic micro/nanoscale plates under linearly varying in-plane load via nonlocal continuum mechanics," Composite Structures, 94(5), 1605-1615(2012).
[9] T. Tai and D. HoChoi, "size-dependent functionally graded kirchhoff and mindlin plate theory based on a modified couple stress theory," Composite Structures, 95,142-153(2013).
[10] B. Akgoz, Omer Civalek, "Free vibration analysis for single –layered graphene sheets in an elastic matrix via modified couple stress theory," materials and design 42, 164-171(2012).
[11] B. Wang, S. Zhou, J. Zhao and X. Chen, "A size-dependent kirchhoff micro-plate model based on strain gradient elasticity theory," European Journal of mechanics

A/Solids, 30(4), 517-524(2011).

[12] C. M. C. Roque, A. J. M. Ferreira and J. N. Reddy, "Analysis of mindlin micro plates with a modified couple stress theory and meshlessmethod," Applied Mathematical Modeling, 37(7), 4626-4633(2013).

[13] Y. G. Wang, W. H. Lin, and N. Liu, "Nonlinear bending and post-buckling of extensible microscale beams based on modified couple stress theory," Applied Mathematical Modeling, 39(1), 117-127(2015).

[14] J. Lei, Y. He, B. Zhang, D. Liu, L. Shen, and S. Guo, "A size-dependent FG micro-plate model incorporating higher-order shear and normal deformation effects based on a modified couple stress theory," International Journal of Mechanical Sciences, 104, 8-23(2015).

[15] H. T. Thai and S. E. Kim, "A size-dependent functionally graded Reddy plate model based on a modified couple stress theory," Composites Part B: Engineering, 45(1), 1636-1645(2013).

[16] B. Akgöz and Ö. Civalek, "Strain gradient elasticity and modified couple stress models for buckling analysis of axially loaded micro-scaled beams," International Journal of Engineering Science, 49(1), 1268-1280(2011).

[17] Y. Chandra, R. Chowdhury, S. Adhikari, and F. Scarpa, "Elastic instability of bilayer graphene using atomistic finite element," Physica E: Low-dimensional Systems and Nanostructures, 44(1), 12-16(2011).

[18] S. Sahmani and R. Ansari, "On the free vibration response of functionally graded higher-order shear deformable microplates based on the strain gradient elasticity theory," Composite Structure, 95, 430–442(2013).

[19] Daghigh, H., Daghigh, V., Milani, A., Tannant, D., Lacy, T. E., Reddy, J. N, Nonlocal bending and buckling of agglomerated CNT-Reinforced composite nanoplates. Composites Part B: Engineering, Vol.183, 107716, (2020).

[20] Daikh, A. A., Houari, M. S. A., & Eltaher, M. A, A novel nonlocal strain gradient Quasi-3D bending analysis of sigmoid functionally graded sandwich nanoplates. *Composite* Structures, In Press, 113347, (2020).

[21] Ruocco, E., & Reddy, J. N, Buckling analysis of elastic–plastic nanoplates resting on a Winkler–Pasternak foundation based on nonlocal third-order plate theory. International Journal of Non-Linear Mechanics, Vol.121, 103453, (2020).

[22] Banh-Thien, T., Dang-Trung, H., Le-Anh, L., Ho-Huu, V., & Nguyen-Thoi, T., Buckling analysis of non-uniform thickness nanoplates in an elastic medium using the isogeometric analysis. Composite Structures, Vol.162, pp.182-193, (2017).

APPENDIX. A

$$E_1 = \frac{\partial^2 w}{\partial x^2}\left[(\lambda+2\mu)(C_3 - C_1 C_2) + \frac{1}{2}\mu l^2(1+C_4) - \frac{1}{4}\mu l^2(1+C_4)(1-C_4)\right] + \frac{\partial^2 w}{\partial y^2}\left[\lambda(C_3 - C_1 C_2) - \frac{1}{2}\mu l^2(1+C_4) + \frac{1}{4}\mu l^2(1-C_4)(1+C_4)\right] + \frac{\partial \varphi_x}{\partial x}\left[-(\lambda+2\mu)(C_2 C_1) - \frac{1}{4}\mu l^2(1-C_4)(1+C_4)\right] + \frac{\partial \varphi_y}{\partial y}\left[-\lambda(C_2 C_1) - \frac{1}{4}\mu l^2(1-C_4)(1+C_4)\right] \tag{A-1}$$

$$E_2 = \frac{\partial^2 w}{\partial y^2}\left[(\lambda+2\mu)(C_3 - C_1 C_2) + \frac{1}{2}\mu l^2(1+C_4) - \frac{1}{4}\mu l^2(1+C_4)(1-C_4)\right] + \frac{\partial^2 w}{\partial x^2}\left[\lambda(C_3 - C_1 C_2) - \frac{1}{2}\mu l^2(1+C_4) + \frac{1}{4}\mu l^2(1-C_4)(1+C_4)\right] + \frac{\partial \varphi_y}{\partial y}\left[-(\lambda+2\mu)(C_2 C_1) - \frac{1}{4}\mu l^2(1-C_4)(1+C_4)\right] + \frac{\partial \varphi_x}{\partial x}\left[-\lambda(C_2 C_1) - \frac{1}{4}\mu l^2(1-C_4)(1+C_4)\right] \tag{A-2}$$

$$E_3 = \frac{\partial^2 w}{\partial x \partial y}\left[4\mu C_2^2 + \mu l^2(1+C_4)^2\right] + \frac{\partial \varphi_x}{\partial y}\left[-2\mu C_2 C_1 - \frac{1}{2}\mu l^2(1-C_4)(1+C_4)\right] + \frac{\partial \varphi_y}{\partial x}\left[-2\mu C_2 C_1 - \frac{1}{2}\mu l^2(1-C_4)(1+C_4)\right] \tag{A-3}$$

$$E_4 = \left(\frac{\partial w}{\partial x}+\varphi_x\right)\left[\mu(1-C_4)^2 + \frac{1}{4}\mu l^2 C_5^2\right] + \left(\frac{\partial^2 \varphi_y}{\partial x \partial y} - \frac{\partial^2 \varphi_x}{\partial y^2}\right)\left[\frac{1}{4}\mu l^2 C_5 C_1\right] \tag{A-4}$$

$$E_5 = \left(\frac{\partial w}{\partial y}+\varphi_y\right)\left[\mu(1-C_4)^2 + \frac{1}{4}\mu l^2 C_5^2\right] + \left(\frac{\partial^2 \varphi_x}{\partial x \partial y} - \frac{\partial^2 \varphi_y}{\partial x^2}\right)\left[\frac{1}{4}\mu l^2 C_5 C_1\right] \tag{A-5}$$

$$E_6 = E_8 = \left(\frac{\partial w}{\partial x}+\varphi_x\right)\left[\frac{1}{4}\mu l^2 C_5 C_1\right] + \left(\frac{\partial^2 \varphi_y}{\partial x \partial y} - \frac{\partial^2 \varphi_x}{\partial y^2}\right)\left[\frac{1}{4}\mu l^2 C_1^2\right] \tag{A-6}$$

$$E_7 = E_9 = \left(\frac{\partial w}{\partial y}+\varphi_y\right)\left[-\frac{1}{4}\mu l^2 C_5 C_1\right] + \left(\frac{\partial^2 \varphi_y}{\partial x^2} - \frac{\partial^2 \varphi_x}{\partial x \partial y}\right)\left[\frac{1}{4}\mu l^2 C_1^2\right] \tag{A-7}$$

$$E_{10} = \frac{\partial^2 w}{\partial x^2}\left[(\lambda+2\mu)(C_1^2 - zC_1) - \frac{1}{4}\mu l^2(1-C_4)(1+C_4)\right] + \frac{\partial^2 w}{\partial y^2}\left[\lambda C_1(-z+C_1) + \frac{1}{4}\mu l^2(1-C_4)(1+C_4)\right] + \frac{\partial \varphi_x}{\partial x}\left[(\lambda+2\mu)C_1^2 + \frac{1}{4}\mu l^2(1-C_4)^2\right] + \frac{\partial \varphi_y}{\partial y}\left[\lambda C_1^2 - \frac{1}{4}\mu l^2(1-C_4)^2\right] \tag{A-8}$$

$$E_{11} = \frac{\partial^2 w}{\partial y^2}\left[(\lambda+2\mu)(C_1^2 - zC_1) - \frac{1}{4}\mu l^2(1-C_4)(1+C_4)\right] + \frac{\partial^2 w}{\partial x^2}\left[\lambda A_1(-z+C_1) + \frac{1}{4}\mu l^2(1-C_4)(1+C_4)\right] + \frac{\partial \varphi_y}{\partial y}\left[(\lambda+2\mu)C_1^2 + \frac{1}{4}\mu l^2(1-C_4)^2\right] + \frac{\partial \varphi_x}{\partial x}\left[\lambda C_1^2 - \frac{1}{4}\mu l^2(1-C_4)^2\right] \tag{A-9}$$

$$E_{12} = \frac{\partial^2 w}{\partial x \partial y}\left[-2\mu C_2 C_1 - \frac{1}{2}\mu l^2(1-C_4)(1+C_4)\right] + \frac{\partial \varphi_x}{\partial y}\left[\mu C_1^2 + \mu l^2(1-C_4)^2\right] + \frac{\partial \varphi_y}{\partial x}\left[\mu C_1^2 - \frac{1}{2}\mu l^2(1-C_4)^2\right] \tag{A-10}$$

$$E_{13} = \frac{\partial^2 w}{\partial x \partial y}\left[-2\mu C_2 C_1 - \frac{1}{2}\mu l^2(1-C_4)(1+C_4)\right] + \frac{\partial \varphi_y}{\partial y}\left[\mu C_1^2 - \frac{1}{2}\mu l^2(1-C_4)^2\right] + \frac{\partial \varphi_y}{\partial x}\left[\mu C_1^2 + \mu l^2(1-C_4)^2\right] \tag{A-11}$$

$$E_{14} = \left(\frac{\partial w}{\partial x}+\varphi_x\right)\left[\mu(1-C_4)^2 + \frac{1}{4}\mu l^2 C_5^2\right] + \left(\frac{\partial^2 \varphi_y}{\partial x \partial y} - \frac{\partial^2 \varphi_x}{\partial y^2}\right)\left[\frac{1}{4}\mu l^2 C_5 C_1\right] \tag{A-12}$$

$$E_{15} = \left(\frac{\partial w}{\partial y}+\varphi_y\right)\left[\mu(1-C_4)^2 + \frac{1}{4}\mu l^2 C_5^2\right] + \left(\frac{\partial^2 \varphi_x}{\partial x \partial y} - \frac{\partial^2 \varphi_y}{\partial x^2}\right)\left[\frac{1}{4}\mu l^2 C_5 C_1\right] \tag{A-13}$$

Where:

$$C_1 = z - \frac{4}{3}\left(\frac{1}{h}\right)^2 z^3 \tag{A-14}$$

$$C_2 = \frac{4}{3}\left(\frac{1}{h}\right)^2 z^3 \tag{A-15}$$

$$C_3 = \frac{4}{3}\left(\frac{1}{h}\right)^2 z^4 \tag{A-16}$$

$$C_4 = 4\left(\frac{z}{h}\right)^2 \tag{A-17}$$

$$C_5 = -8z\left(\frac{1}{h}\right)^2 \tag{A-18}$$

$$C_6 = \frac{4}{3}\left(\frac{1}{h}\right)^2 \tag{A-19}$$

$$C_7 = \mu\frac{h}{3} \tag{A-20}$$

$$C_8 = \mu\frac{h}{5} \tag{A-21}$$

$$C_9 = \frac{h^3}{252}(\lambda + 2\mu) \tag{A-22}$$

$$C_{10} = (\lambda + 2\mu)\frac{h^3}{60} \tag{A-23}$$

$$C_{11} = \mu\, l^2\frac{4}{3h} \tag{A-24}$$

$$C_{12} = \frac{1}{4}\mu\, l^2 h \tag{A-25}$$

APPENDIX. B

$$D_1 = 2C_{12} + l^2 C_7 + \frac{1}{2}l^2 C_8 + 2C_9 \tag{B-1}$$

$$D_2 = \frac{1}{2}D_1 = C_{12} + C_9 + \frac{1}{2}l^2 C_7 + \frac{1}{4}l^2 C_8 \tag{B-2}$$

$$D_3 = -\mu h + 2C_7 - C_8 - C_{11} \tag{B-3}$$

$$D_4 = C_9 - C_{10} + \frac{1}{4}l^2 C_8 - C_{12} \tag{B-4}$$

$$D_5 = 3C_{12} - \frac{3}{2}l^2 C_7 + \frac{3}{4}l^2 C_8 - (\lambda + \mu)I_2 + 2(\lambda + \mu)C_6 I_4 \\ - (\lambda + \mu)C_6{}^2 I_6 \tag{B-5}$$

$$D_6 = -\mu I_2 + 2\mu C_6 I_4 - \mu C_6{}^2 I_6 - 4C_{12} + 2l^2 C_7 - l^2 C_8 \tag{B-6}$$

$$D_7 = \frac{1}{4}\mu l^2 I_2 - \frac{1}{2}\mu l^2 C_6 I_4 + \frac{1}{4}\mu l^2 C_6{}^2 I_6 \tag{B-7}$$

$$D_8 = -(\lambda + 2\mu)I_2 + 2C_{10} - C_9 - C_{12} + \frac{1}{2}l^2 C_7 - \frac{1}{4}l^2 C_8 \tag{B-8}$$

$$D_9 = \frac{5}{4}l^2 C_8 - \frac{3}{2}\mu l^2 C_6{}^2 I_4 - \frac{5}{2}l^2 C_7 + 3C_{12} - (\lambda + \mu)I_2 \\ - (\lambda + \mu)C_6{}^2 I_6 + 2(\lambda + \mu)C_6 I_4 \tag{B-9}$$

$$D_{10} = 3l^2 C_7 - \frac{3}{2}l^2 C_8 + \frac{3}{2}\mu l^2 C_6{}^2 I_4 - \mu I_2 - \mu C_6{}^2 I_6 + 2\mu C_6 I_4 \\ - 4C_{12} \tag{B-10}$$

$$D_{11} = \rho C_6{}^2 I_6 \tag{B-11}$$

$$D_{12} = \rho C_6 I_4 - \rho C_6{}^2 I_6 \tag{B-12}$$

$$D_{13} = \rho I_2 - 2\rho C_6 I_4 - \rho C_6{}^2 I_6 \tag{B-13}$$

APPENDIX. C

$$R_1 = D_1\alpha^2\beta^2 + D_2\alpha^4 + D_2\beta^4 - D_3\alpha^2 - D_3\beta^2 - P_x\alpha^2 \\ - P_y\beta^2 \tag{C-1}$$

$$R_2 = R_4 = D_4\alpha^3 + D_4\alpha\,\beta^2 - D_3\alpha \tag{C-2}$$

$$R_3 = R_7 = D_4\beta^3 + D_4\alpha^2\beta - D_3\beta \tag{C-3}$$

$$R_5 = -D_7\beta^4 - D_7\alpha^2\beta^2 - D_6\beta^2 - D_8\alpha^2 - D_3 \tag{C-4}$$

$$R_6 = D_7\alpha\beta^3 + D_7\alpha^3\beta - D_5\alpha\beta \tag{C-5}$$

$$R_8 = -D_7\alpha^3\beta - D_7\alpha\beta^3 - D_9\alpha\beta \tag{C-6}$$

$$R_9 = D_7\,\alpha^4 + D_7\alpha^2\beta^2 - D_{10}\alpha^2 - D_8\beta^2 - D_3 \tag{C-7}$$

$$G_1 = -D_{11}\alpha^2 - D_{11}\,\beta^2 - \rho h \tag{C-8}$$

$$G_2 = G_4 = D_{12}\alpha \tag{C-9}$$

$$G_3 = G_7 = D_{12}\beta \tag{C-10}$$

$$G_5 = G_9 = -D_{13} \tag{C-11}$$

$$G_6 = G_8 = 0 \tag{C-12}$$